Beyond the primary site: Molecular insights and clinical implications of cancer metastatic overlap between lung and urological organ cancers (Review)

YINHUAN WANG[1] and JIEFANG GUAN[2]

[1]Department of Urology, The Third Affiliated Hospital of Gansu University of Chinese Medicine, Baiyin, Gansu 730900, P.R. China; [2]Department of Thoracic Surgery, The Third Affiliated Hospital of Gansu University of Chinese Medicine, Baiyin, Gansu 730900, P.R. China

Received November 25, 2025; Accepted March 23, 2026

DOI: 10.3892/mmr.2026.13924

Abstract. Metastasis between primary lung cancers and urological malignancies, for example prostate, renal and bladder cancers, poses diagnostic and therapeutic challenges. Previous epidemiological data underscore a frequent bidirectional overlap that adversely affects patient survival. This review synthesizes current molecular insights and clinical implications of this metastatic crosstalk, delineating how these distinct tumor types exploit shared molecular toolkits, including the C-X-C chemokine receptor 4/C-X-C motif chemokine ligand 12 axis, hepatocyte growth factor/mesenchymal-epithelial transition factor signaling and epithelial-mesenchymal plasticity, to facilitate dissemination and colonization. The distinct immune contextures and cellular architectures of the metastatic niche in different organs have also been explored, revealing their notable influence on therapeutic responses. Although molecular profiling and liquid biopsies have been refining diagnostic precision and allowing for a shift toward mechanism-centric agnostic therapies, organ-specific microenvironments continue to modulate drug efficacy. Integration of these insights is necessary for advancing personalized management strategies and improving outcomes for patients in this complex clinical setting.

Contents

Correspondence to: Dr Jiefang Guan, Department of Thoracic Surgery, The Third Affiliated Hospital of Gansu University of Chinese Medicine, 222 Silong Road, Baiyin, Gansu 730900, P.R. China
E-mail: 15209435958@163.com

Abbreviations: CAFs, cancer-associated fibroblasts; CAR-T, chimeric antigen receptor T-cell; ctDNA, circulating tumor DNA; dMMR, mismatch-repair deficient; EMT, epithelial-mesenchymal transition; FAP, fibroblast activation protein; ICIs, immune-checkpoint inhibitors; MDT, multidisciplinary team; MET, mesenchymal-epithelial transition; MSI-H, microsatellite instability-high; NSCLC, non-small cell lung cancer; PARP, poly(ADP-ribose) polymerase; PD-L1, programmed death-ligand 1; RCC, renal cell carcinoma; TAMs, tumor-associated macrophages; TLS, tertiary lymphoid structure; TMB, tumor mutational burden; TME, tumor microenvironment

Key words: organotropism, metastatic niche, lung cancer, urological cancers, liquid biopsy, TME, targeted therapy

1. Introduction

Metastatic disease remains the predominant determinant of cancer-related mortality, and previous population-based analyses indicate that bidirectional dissemination of cancer cells between the lungs and urological organs is more frequent than previously appreciated (1). A study by Deng *et al* (1) reported that, based on data from the Surveillance, Epidemiology and End Results database (SEER) (2), 18.4% of patients with *de novo* metastatic prostate adenocarcinoma presented with pulmonary involvement. In this analysis, bone represented the most common metastatic site, whereas pulmonary involvement was associated with a distinct prognostic disadvantage. This subset exhibited a median overall survival (OS) that was 7.3 months shorter than that of patients with bone-only disease, even after adjustment for age and Gleason score. The Gleason scoring system is the standardized histopathological grading system for prostate adenocarcinoma, ranging from 6 to 10, with higher scores indicating poorer differentiation and more aggressive disease (3). Comparable patterns of dissemination have been documented for renal cell carcinoma (RCC); a study reported by Wei *et al* (4) investigated 47,555 RCC cases diagnosed

between 2010 and 2018 and reported that isolated lung-only metastases, defined as lung involvement without concurrent metastases to other organs, were detected in 22.1% of patients, whereas isolated visceral metastases in the kidney, adrenal gland or bladder derived from primary lung cancers constituted 4.6% of all lung-cancer deaths. These figures underscore the necessity of considering the pulmonary-urological axis as a clinically important yet underappreciated route of metastatic spread. As detailed in Table I (1,4-6), these epidemiological findings have revealed distinct prognostic sub-features that complicate clinical management. For example, patients aged <55 years paradoxically have poorer survival outcomes of prostate-to-lung metastasis (1), whereas histological dedifferentiation, as evidenced by the presence of sarcomatoid features, completely abolishes therapeutic benefits in renal-to-lung disease (4). Notably, the concept of metastatic overlap within this axis is clinically heterogeneous. In the present study, this term has been defined to encompass three distinct scenarios: i) True cross-organ metastasis; ii) multiple synchronous primary malignancies (7); and iii) the rare phenomenon of tumor-to-tumor metastasis (8).

Despite the epidemiological importance of this metastatic overlap, accurate differentiation between the aforementioned three scenarios, namely true cross-organ metastasis, multiple synchronous primary malignancies and tumor-to-tumor metastasis, at the pulmonary-urological anatomical interface remains challenging. Conventional imaging techniques frequently fail to discriminate between *de novo* pulmonary neoplasms and urological metastases, which is particularly evident in cases involving solitary lesions. In a multi-institutional series of 312 patients with clear-cell RCC (ccRCC) that developed lung nodules after nephrectomy, 18% of cases were ultimately re-classified as synchronous primary non-small cell lung cancer (NSCLC) following targeted sequencing, leading to notable changes in the systemic therapy strategies used, as treatment shifted from RCC-directed regimens (e.g., vascular endothelial growth factor or mammalian target of rapamycin inhibitors) to NSCLC-specific approaches (e.g., tyrosine kinase inhibitors or immune-checkpoint blockade) (7). Conversely, tumor-to-tumor metastasis from prostate adenocarcinoma into an incumbent lung adenocarcinoma has been documented, further blurring histogenic boundaries (8). The resultant diagnostic uncertainty of tumors along this axis translates into therapeutic delays; data from SCRUM-Japan MONSTAR SCREEN project, a large-scale cancer genomic screening initiative showed that the median duration from radiological suspicion of tumor identity to tissue confirmation was 42 days longer when urological and lung pathology overlapped than when metastases occurred within the same organ system (5). In this cohort, isolated visceral metastases in the kidney derived from primary NSCLC accounted for 4.6% of all lung-cancer deaths, and solitary renal lesions in this setting were frequently misclassified as second primary tumors, further complicating clinical decision-making (5).

Molecular profiling has begun to clarify whether the appearance of additional tumors along the lung-urological axis represents genuine cross-organ colonization or the emergence of an anatomically adjacent second primary. In a study reported by Steindl *et al* (9), whole-exome sequencing was performed on 28 primary RCC samples and paired brain or lung metastases; the study observed a mean Jaccard index value of 0.78 for shared mutations, indicating that metastases were the result of monoclonal dissemination. Similar clonality was observed in prostate cancer: In a study reported by Shiota *et al* (5), ctDNA was analyzed from 194 patients with castration-resistant prostate cancer enrolled in the SCRUM-Japan MONSTAR SCREEN project. The study found that the same androgen receptor (AR)-ligand binding-domain alteration detected in primary tumors was present in 86% of concurrent pulmonary metastases, whereas this modification was absent in 12 of 13 synchronous primary lung cancers identified in the same cohort. These findings supported the concept of molecular convergence, in which distinct primary tumors exploit common signaling axes, such as the C-X-C chemokine receptor (CXCR)4/C-X-C motif chemokine ligand (CXCL)12, hepatocyte growth factor (HGF)/mesenchymal-epithelial transition factor (c-MET) and tyrosine-protein kinase receptor UFO/growth arrest-specific protein 6 pathways, to establish pulmonary or urological sanctuary sites (10,11).

The therapeutic implications of this molecular overlap have been well-documented. A study reported by Furubayashi *et al* (6) retrospectively evaluated 92 patients with metastatic urothelial carcinoma who received the immune-checkpoint inhibitor (ICI) pembrolizumab after platinum failure; objective response rates (ORRs) in lung lesions mirrored those in lymph-node sites, which were observed to be 38 and 35% respectively, whereas renal parenchymal lesions responded to treatment in only 14% of cases. In this study, lung metastases were present in 15.6% of patients following platinum-based chemotherapy failure, and a programmed death-ligand 1 (PD-L1) combined positive score (CPS) of ≥10 was associated with a marked improvement in ORR, increasing from 38 to 68% in this subgroup (6). These findings suggested that the pulmonary microenvironment may be particularly amenable to immune-checkpoint blockade. Conversely, targeted agents conventionally restricted to NSCLC have shown notable activity in urological metastases. Treatment with the MET inhibitor savolitinib induced a partial response in 42% of pulmonary metastases arising from papillary RCC in a single-arm phase II trial, a value that parallels the 44% response rate observed in primary lung tumors harboring *MET* exon 14 skipping alterations (12). Such findings exemplify the shift from organ-centric to mechanism-centric therapy and highlight the necessity for robust biomarkers that can reliably identify tumor origin.

Emerging technologies have shown promise in resolving this diagnostic bottleneck, namely the difficulty in accurately distinguishing between primary lung neoplasms and urological metastases when lesions present along the pulmonary-urological axis. In a study reported by Wang *et al* (13), a 10-CpG locus methylation classifier was developed using ctDNA that distinguished pulmonary metastases of RCC from primary NSCLC tumors with an area under the curve (AUC) value of 0.92, outperforming the classical transcription termination factor 1 (TTF-1)/paired box 8 (PAX8) immunohistochemistry (IHC) panel (AUC, 0.79). Furthermore, single-cell RNA sequencing has revealed metastatic trajectory-specific signatures. CD103-positive cancer stem cell-derived exosomes

Table I. Epidemiological profile of metastatic overlap between primary lung and urological cancers.

First author, year	Primary tumor	Metastatic direction	Incidence among m-stage patients	Key prognostic sub-features	(Refs.)
Deng *et al*, 2019	Prostate adenocarcinoma	Lung	18.4%	The patients aged <55 years with prostate-to-lung metastasis were classified as the 'younger' subgroup; this subgroup paradoxically exhibited shorter overall survival compared with older patients, particularly in the presence of non-bone co-metastasis.	(1)
Wei *et al*, 2021	Clear-cell renal cell carcinoma	Lung-only	22.1%	Sarcomatoid dedifferentiation abolishes therapeutic benefits.	(4)
Shiota *et al*, 2025	Primary NSCLC	Kidney	4.6% of all lung-cancer mortalities	Solitary renal lesions are frequently misclassified as second primary tumors.	(5)
Furubayashi *et al*, 2021	Urothelial carcinoma	Lung	15.6% following platinum-based chemotherapy failure	PD-L1 CPS≥10 almost doubles ORR from 38 to 68%.	(6)

OS, overall survival; m-stage, metastatic stage; NSCLC, non-small cell lung cancer; RCC, renal cell carcinoma; CPS, combined positive score; ORR, objective response rate; PD-L1, programmed death-ligand 1.

enriched in microRNA (miR)-19b-3p have been shown to prime pulmonary endothelial cells for metastatic docking in ccRCC, whereas miR-210-3p-enriched exosomes derived from prostate cancer favored renal cortical colonization (13,14). These approaches are orthogonal in that the 10-CpG methylation classifier provides a diagnostic tool based on epigenetic DNA modifications, whereas exosomal miRNA profiling offers mechanistic insights into non-coding RNA-mediated metastatic signaling; together, these orthogonal approaches not only refine current insights into metastatic organotropism but also provide non-invasive platforms for longitudinal monitoring.

In summary, epidemiological data have demonstrated that bidirectional metastatic spread between the lungs and urological organs is common and prognostically important, yet recognition of this event is hampered by inherent diagnostic ambiguity. Molecular evidence has indicated that metastasis of this nature frequently represents genuine clonal dissemination driven by shared genomic and epigenetic programs. Integrating these molecular insights with evolving liquid-biopsy technologies offers a rational framework for early detection, precise tumor identification and mechanism-based therapies, which represents an imperative step towards improving outcomes in this challenging clinical scenario.

2. Hallmarks of metastasis: A shared toolkit for dissemination

Irrespective of primary organ, metastatic progression follows a stereotypical sequence: i) Local invasion; ii) intravasation; iii) survival in circulation; iv) extravasation; and v) secondary colonization. Accumulating evidence indicates that lung and urological cancers exploit the same functional modules during these steps (15-17). This implies that therapeutic interception of the shared toolkit may confer cross-organ efficacy. Table II (15-24) juxtaposes the activity of specific molecular effectors, such as profilin-2 in lung cancer and circPRRC2A in renal cancer, in pulmonary and urological cancers to demonstrate how distinct molecules achieve identical functional outcomes, such as vascular permeability and immune evasion, across different tumor types.

Invasion and epithelial-mesenchymal transition (EMT). EMT constitutes a conserved molecular switch that confers motility and proteolytic capacity (15). In prostate cancer, AR loss in epithelial cells activates TGF-β1 signaling, leading to classical E-cadherin downregulation and vimentin upregulation; this shift has been shown to increase pulmonary seeding of metastases in castration-resistant models (15). Concordantly, NSCLC cells that overexpress neuronal acetylcholine receptor α5 (α5-nAChR) have been shown to trigger Jun activation domain-binding protein 1 (Jab1)-mediated EMT, accelerating renal parenchymal colonization (18). Although the upstream inducers differ (TGF-β1 in prostate cancer vs. α5-nAChR/Jab1 in lung cancer), the downstream transcriptional effectors converge on shared regulators of EMT, including TGF-β, Jab1 and Snail (encoded by SNAI1), which operate in both directions of the lung-urological axis.

Despite this convergence, transitional kinetics differ. Prostate tumors display a gradual EMT trajectory that permits micrometastatic dormancy within alveoli, whereas EGFR-mutant lung adenocarcinoma has been shown to undergo a rapid, complete transition, which facilitates immediate renal cortical infiltration (25). Such temporal heterogeneity is attributable to lineage-specific chromatin landscapes (25), but the downstream EMT effectors remain shared. Clinically, this dictates that the timing of EMT-targeted therapies must

Table II. Shared metastatic toolkit in lung and urological cancers.

Metastatic step	Core mechanism	Examples in lung cancer	Examples in urological cancers	(Refs.)
Invasion and EMT	Loss of epithelial features, gain of motility and. invasiveness	α5-nAChR overexpression triggers Jab1-mediated EMT, accelerating renal colonization.	Androgen receptor loss activates TGF-β1 signaling, driving EMT and pulmonary seeding in castration-resistant prostate cancer.	(15,18)
Intravasation and CTCs	Penetration of the endothelial barrier to enter circulation.	Profilin-2-enriched exosomes remodel the actin cytoskeleton, promoting intravasation and bone-marrow dissemination.	circPRRC2A-loaded exosomes downregulate TIMP2 and activate VEGFA/VEGFR2 signaling, enhancing vascular permeability in ccRCC.	(16,19)
CTC survival	Evasion of shear stress and immune surveillance in circulation.	Resveratrol restores NK-cell cytotoxicity, diminishing CTC viability in a melanoma lung-metastasis model.	Cathepsin K blockade suppresses IL-17-mediated EMT and polarizes macrophages from the M2 to M1 phenotype, reducing lung metastasis in prostate cancer.	(17,20)
Extravasation	Exit from the vasculature at the distant site.	Bevacizumab, an anti-VEGF therapeutic agent, normalizes tight junctions, attenuating brain extravasation.	Inhibition of apelin/APJ signaling stabilizes tight junctions, reducing renal cortex extravasation of prostate CTCs.	(21,22)
Colonization and MET	Re-establishment of epithelial features to proliferate and form metastases.	The PP4R1-HMGA2 interactionsustains ERK-dependent EMT, accelerating renal metastasis; ERK inhibition restores the epithelial phenotype.	KLF5-mediated MET enables prostate cancer cells to proliferate within pulmonary alveoli after dissemination.	(23,24)

EMT, epithelial-mesenchymal transition; MET, mesenchymal-epithelial transition; CTCs, circulating tumor cells; ccRCC, clear-cell renal cell carcinoma; VEGF, vascular endothelial growth factor; VEGFR2, vascular endothelial growth factor receptor 2; α5-nAChR, neuronal acetylcholine receptor α5; Jab1, Jun activation domain-binding protein 1; NK, natural killer; TIMP2, tissue inhibitor of metalloproteinases 2; APJ, apelin receptor; KLF5, Krüppel-like factor 5; PP4R1, protein phosphatase 4 regulatory subunit 1; HMGA2, high mobility group AT-hook protein 2.

be synchronized with these distinct kinetic profiles; rapidly transitioning lung tumors likely require upfront, concurrent blockade to prevent immediate seeding, whereas the indolent chromatin states of prostate-derived micrometastases may be more suitably managed via maintenance strategies targeting epigenetic plasticity.

Intravasation and circulating tumor cells (CTCs). Once cancer cells acquire motility, they penetrate the endothelial barrier. Small-cell lung cancer-derived exosomes are enriched in profilin-2, which remodels the actin cytoskeleton of recipient cancer cells, promoting intravasation and subsequent bone marrow dissemination (19). A parallel mechanism has been observed in ccRCC, in which circPRRC2A-loaded exosomes increase vascular permeability by downregulating tissue inhibitor of metalloproteinases 2 and activating the vascular endothelial growth factor (VEGF)A/VEGF receptor (VEGFR)2 axis (16). In both studies, functional read-outs, including enhanced trans-endothelial migration and increased circulating tumor cell (CTC) counts, were observed, confirming a shared exosome-mediated intravasation gateway (16,19).

Survival in circulation. CTCs are subject to both shear stress and immune surveillance in circulation. In a melanoma lung-metastasis model, resveratrol has been shown to diminish CTC viability by restoring natural killer (NK)-cell cytotoxicity (20). Similarly, cathepsin K blockade in castration-resistant prostate cancer has been found to suppress IL-17-mediated EMT and reduce lung metastasis by polarizing M2 macrophages towards an M1 phenotype (17). Collectively, these findings imply that immunomodulatory checkpoints, notably programmed death-ligand 1 (PD-L1), constitute a conserved 'survival module' for CTCs of divergent origins.

Extravasation and endothelial activation. Exit from the vasculature requires endothelial activation. Bevacizumab-mediated VEGF blockade has been shown to attenuate brain extravasation of lung cancer cells by normalizing tight-junction architecture (21). Similarly, inhibition of apelin/apelin receptor signaling has been shown to reduce renal cortex extravasation of prostate CTCs through the same junctional stabilization mechanism (22). Targeting VEGFs or their cognate receptors therefore constitutes a cross-organ strategy for impeding extravasation in the lung-urological metastatic route.

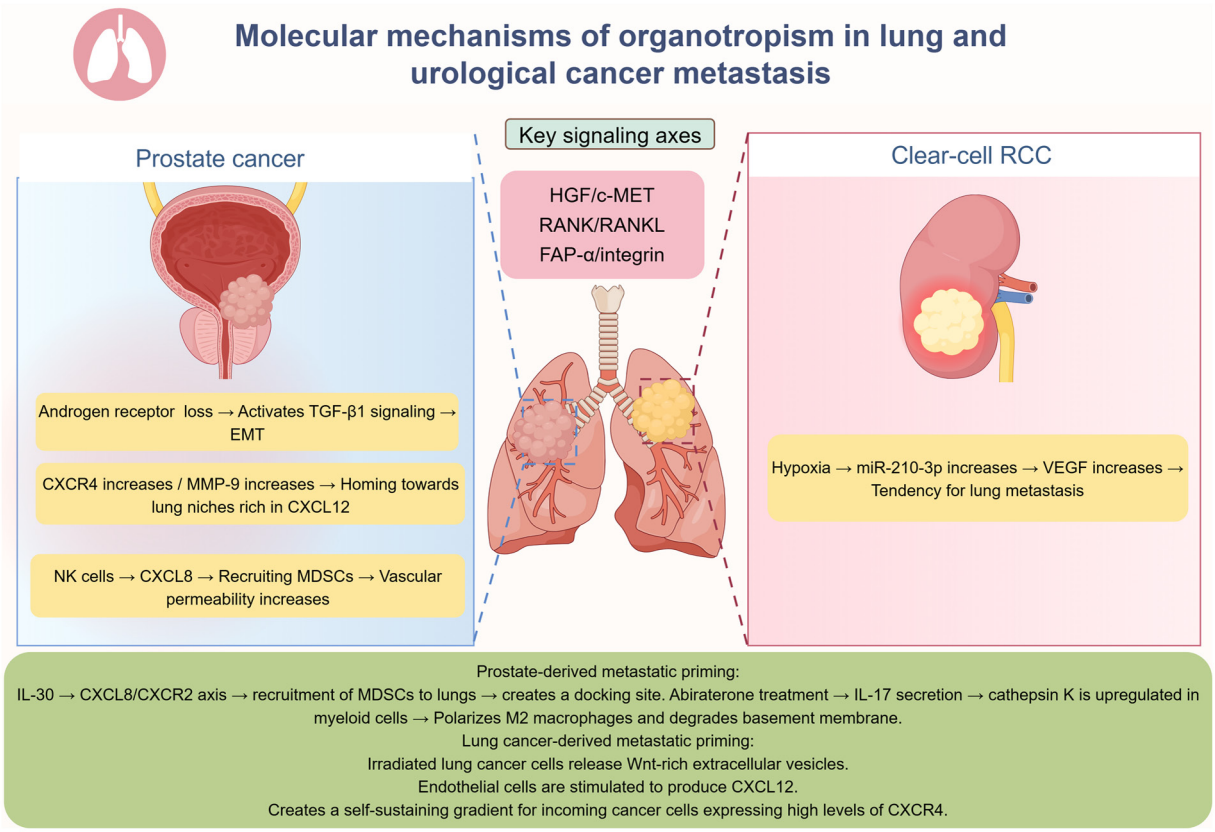

Figure 1. Molecular drivers of site-specific tropism in lung and urological metastases. EMT, epithelial-mesenchymal transition; HGF, hepatocyte growth factor; c-MET, mesenchymal-epithelial transition factor; RANK, receptor activator of NF-κB; RANKL, receptor activator of NF-κB ligand; FAP-α, fibroblast activation protein-α; CXCR, C-X-C chemokine receptor; MMP-9, matrix metalloproteinase-9; CXCL, C-X-C motif chemokine ligand; MDSC, myeloid-derived suppressor cell; NK, natural killer; miR, microRNA; VEGF, vascular endothelial growth factor. The figure was created with Figdraw (www.figdraw.com).

Colonization and reversible MET. Successful colonization hinges on tumor cells re-establishing epithelial characteristics via MET. In lung adenocarcinoma, the protein phosphatase 4 regulatory subunit 1-high mobility group AT-hook protein 2 interaction has been shown to sustain ERK-dependent EMT and accelerate renal parenchymal metastasis; conversely, ERK inhibition restores the epithelial phenotype and reduces colonization (23). Concordantly, prostate cancer cells utilize Krüppel-like factor 5-mediated MET to proliferate within pulmonary alveoli after initial dissemination (24). The reversibility of EMT has therefore emerged as a shared attribute of metastatic colonization along the lung-urological axis (26). However, the duration required for MET to occur differs between tumor types, underscoring the need for lineage-specific scheduling of EMT-targeting agents.

3. Molecular drivers of site-specific tropism

Molecular determinants of metastatic site preference between lung and urological cancers collectively involve the TGF-β1/EMT, CXCR4/CXCL12, HGF/c-MET and CXCL8/CXCR2 signaling axes. Notably, the CXCR4/CXCL12 and CXCL8/CXCR2 axes are predominantly engaged in pulmonary tropism (from urological primaries to the lung), whereas the HGF/c-MET and TGF-β1/EMT axes mediate bidirectional signaling, collectively establishing site-specific tropism through lineage-specific exosomal cargo and stromal reprogramming (9,26). These reciprocal tropism pathways represent potential therapeutic targets and have been graphically summarized in Fig. 1. This figure visually reconstructs the 'seed and soil' interaction, contrasting the intrinsic 'seed' factors, such as CXCR4 upregulating and miR-210 secretion, against the 'soil' priming mechanisms, for example IL-30-mediated recruitment of myeloid-derived suppressor cells (MDSCs) and fibronectin deposition. By mapping these bidirectional signals, Fig. 1 illustrates how soluble factors and exosomes create a permissive pre-metastatic niche long before macroscopic colonization occurs.

'Seeds': Cancer-cell-intrinsic tropism factors. Prostate cancer deficient in epithelial AR has been shown to switch from an epithelial to a mesenchymal phenotype via TGF-β1-driven EMT, concurrently upregulating CXCR4 and matrix metalloproteinase (MMP)-9; the CXCR4/CXCL12 chemokine-receptor pair guides circulating cells toward pulmonary niches rich in CXCL12 and fibronectin, whereas MMP-9 contributes to extracellular matrix remodeling during invasion (26). Conversely, in NSCLC, CXCR4 upregulating facilitates tropism to the kidney, where renal stromal cells produce CXCL12, creating a permissive niche for metastatic seeding (9,26). This bidirectional evidence establishes the CXCR4/CXCL12 axis as a shared molecular mechanism governing cross-organ dissemination along the lung-urological axis. Peripheral blood NK cells extracted from the same patients have been shown

to amplify CXCL8 secretion, recruiting $CD11b^+$ Grl^+ (Gr-1 is the myeloid differentiation antigen, a classic surface marker for myeloid-derived suppressor cells and granulocytes in mice) MDSCs into alveolar septa and increasing vascular leakiness, therefore providing an ideal docking platform for incoming CTCs (26). In ccRCC, hypoxic regions show an upregulation of secreted miR-210-3p; serum levels of miR-210-3p associate with VEGF concentration and independently predict future pulmonary relapse (14). Thus, both tumor types have been shown to utilize soluble factors, such as CXCL8 or miR-210-3p, to pre-program the homing of CTCs to pulmonary tissues, although the specific molecular cargo differs by lineage: prostate cancer-derived NK cells secrete CXCL8 to recruit MDSCs (26), whereas ccRCC-derived exosomes deliver miR-210-3p to promote angiogenesis and create a permissive pulmonary niche (14).

'Soil': Niche-priming by secreted factors. Once primary tumors reach a critical mass, pre-metastatic 'soil' tissues are primed. As aforementioned, prostate cancer-derived IL-30 recruits $CD11b^+$ Grl^+ MDSCs into alveolar septa via CXCL8/CXCR2 signaling and increases microvascular permeability, creating a pulmonary docking site for incoming CTCs (26). Abiraterone-treated prostate tumors have been shown to secrete IL-17 that upregulates cathepsin K in CD11b+ myeloid cells; cathepsin K in turn polarizes M2 macrophages and degrades the alveolar basement membrane, doubling pulmonary tumor burden in orthotopic mice (27). Conversely, irradiated lung cancer cells secrete Wnt-enriched extracellular vesicles that stimulate neighboring endothelial cells to produce CXCL12, thereby creating a self-sustaining gradient for incoming prostate CTCs exhibiting elevated levels of CXCR4 (28). These findings indicate that bidirectional 'soil' preparation relies on common effector classes, such as cytokines and extracellular vesicles (EVs), even though upstream triggers are tumor-type specific, for example androgen-deprivation (27) vs. radiotherapy (28).

Signaling axes governing cross-organ tropism. Three signaling cascades repeatedly appear in both tropism directions along the pulmonary-urological axis: i) The HGF/c-MET pathway; ii) the receptor activator of NF-κB (RANK)/RANK ligand (RANKL) signaling pathway; and iii) the fibroblast activation protein (FAP)-α/integrin signaling pathway. Functionally, these axes are not redundant with the primary determinants (TGF-β1/EMT, CXCR4/CXCL12 and CXCL8/CXCR2) outlined in the introductory paragraph of this section. Rather, the CXCR4/CXCL12 and TGF-β1/EMT axes serve as the dominant drivers for initial site-specific homing, whereas the HGF/c-MET, RANK/RANKL, and fibroblast activation protein-α (FAP-α)/integrin pathways act as secondary, context-dependent mechanisms that primarily facilitate metastatic niche establishment, colonization, and progression following initial seeding (29,30). Regarding the HGF/c-MET axis, MET amplification in papillary RCC has been shown to increase pulmonary colonization, whereas HGF produced by pulmonary fibroblasts reciprocally stimulates c-MET on NSCLC cells, accelerating renal parenchymal invasion (29). Similarly, osteoblast-derived RANKL has been found to attract prostate cancer cells exhibiting high levels of CXCR4 to bone tissue, whereas RANKL expressed by renal tubular cells has been shown to foster pulmonary metastatic foci (26). Finally, imaging with [68Ga] DATA-conjugated fibroblast activation protein inhibitor (Ga-DATA-FAPi) has shown that FAP-positive cancer-associated fibroblasts (CAFs) are enriched in both lung and renal pre-metastatic sites; pharmacological inhibition of FAP-α decreases tumor cell adherence under flow conditions (30,31). Convergence on these axes suggests that targeting stromal rather than tumoral components may abrogate organotropism regardless of primary tumor location.

However, previous evidence suggests that these axes are not equipotent. Among the multiple signaling axes involved, the CXCR4/CXCL12 axis functions as the predominant homing mechanism for initial metastatic seeding, particularly in prostate-to-lung dissemination, as constitutive high expression of CXCL12 in the pulmonary vasculature universally attracts CXCR4-positive circulating tumor cells (26). Similarly, in lung-to-kidney dissemination, CXCR4-expressing NSCLC cells home to CXCL12-abundant renal stroma, highlighting the shared and reciprocal nature of this signaling axis (9,26). By contrast, the HGF/c-MET pathway represents a more context-dependent signaling mechanism, predominantly driving colonization in specific histological subtypes, such as papillary RCC, or acting as a secondary survival pathway that facilitates progression rather than initial seeding (29). Other axes, including RANK/RANKL and FAP-α/integrin signaling, contribute to niche priming and stromal support but do not serve as primary homing switches (26,30,31).

Therapeutic exploitation of tropic pathways. Cathepsin K inhibition using odanacatib has been shown to curb IL-17-mediated M2 polarization and reduce pulmonary tumor burden in castration-resistant prostate cancer (27). Furthermore, hypoxia-mimetic 19-hydroxybufalin downregulates hypoxia-inducible factor-1α (HIF-1α), subsequently reducing miR-210-3p secretion and attenuating ccRCC-induced angiogenesis (32); this implies that oxygen-sensing modifiers may indirectly blunt lung homing.

Regarding the therapeutic utility of the CXCR4/CXCL12 axis, clinical positron emission tomography (PET) using Ga-pentixafor has demonstrated robust CXCR4 upregulation in pulmonary lesions (33). This imaging biomarker, reflecting CXCR4 expression levels, provides a non-invasive method that may predict responsiveness to future CXCR4-directed therapy in clinical trials targeting prostate cancer or ccRCC. Treatment with a representative quinolinoyl-cyanopyrrolidine inhibitor of FAP-α has been shown to decrease tumor-cell adhesion under physiological flow, and its combination with standard chemotherapy synergistically suppressed tumor growth in lung-cancer xenografts (31,34). Given that FAP-α is predominantly expressed on cancer-associated fibroblasts in the tumor stroma, these findings suggest that stromal targeting can override organ-specific 'soil' signals.

Finally, resveratrol restores NK-cell cytotoxicity and suppresses melanoma lung metastasis by modulating sirtuin-1 and oxidative stress levels (31,35); since hypoxia-driven reactive oxygen species also govern prostate-to-lung CTC trafficking (36), the repurposing of antioxidants as adjuvants may attenuate tropism across the urological-pulmonary axis. Collectively, these proof-of-concept studies support

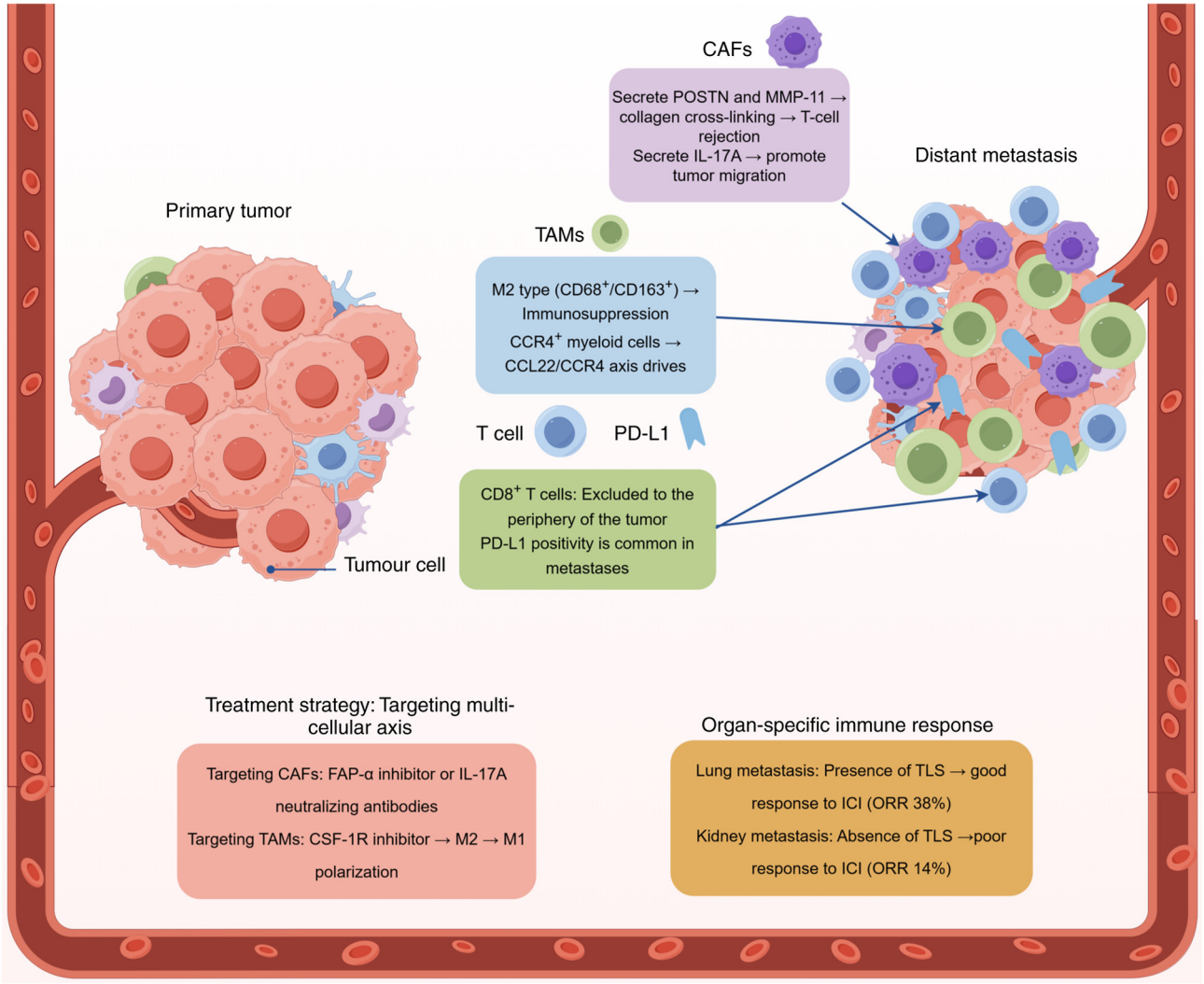

Figure 2. Tumor microenvironment and immune contexture at the metastatic site. CAF, cancer-associated fibroblast; TAM, tumor-associated macrophage; PD-L1, programmed death-ligand 1; FAP-α, fibroblast activation protein-α; CSF-1R, macrophage colony-stimulating factor 1 receptor; TLS, tertiary lymphoid structure; ICI, immune-checkpoint inhibitor; ORR, objective response rate; POSTN, periostin; MMP, matrix metalloproteinase; CCR4, C-C chemokine receptor type 4; CCL22, C-C motif chemokine ligand 22. The figure was created with Figdraw (www.figdraw.com).

the 'seed-and-soil' paradigm and provide evidence that the processes involved in this metastatic route represent notable therapeutic targets, although combination treatments will be required to counteract compensatory signaling and achieve durable blockade of site-specific metastasis.

4. Tumor microenvironment (TME) and immune contexture at the metastatic site

Metastatic seeding in the lung does not involve the passive lodging of tumor cells but rather the active remodeling of the TME, which is orchestrated by CAFs and tumor-associated macrophages (TAMs) that collectively construct an immune-privileged niche. Periostin (POSTN)$^+$ and MMP-11$^+$ CAFs drive collagen cross-linking and T-cell exclusion, whereas hypoxia-educated M2-like TAMs (i.e., TAMs that acquire an immunosuppressive phenotype upon activation by hypoxic conditions) reinforce immunosuppression; the spatial interplay of these cells has been summarized in Fig. 2. This figure highlights the immune-exclusion phenotype (characterized by CD8$^+$ T cells confined to the invasive margins rather than infiltrating the tumor core) characteristic of these metastases, showing how the physical barrier formed by activated CAFs and the functional immune-suppression induced by M2-TAMs collectively prevent CD8$^+$ T-cell infiltration into the tumor core, thereby limiting the efficacy of monotherapy.

Cellular architects of the metastatic niche: CAFs and TAMs. The cellular composition of the metastatic niche is predominantly shaped by CAFs and TAMs. CAFs positive for markers such as α-SMA constitute a notable portion of the stromal area in pulmonary metastases, varying from 25-40%, a frequency comparable with their primary tumors (9). Functionally, these CAFs are not inert, but rather actively promote malignancy. In ccRCC, a subset of CAFs expressing POSTN and MMP-11 has been demonstrated to contribute to collagen cross-linking and T-cell exclusion, creating a physical and biochemical barrier against immune attack (13). This pro-invasive effect, which can inhibitors targeting FAP-α, a key enzyme expressed on CAFs, validates CAFs as a druggable stromal component

across tumor types (37). In prostate cancer, CAFs have been shown to promote malignant progression through autophagy induction and the secretion of pro-inflammatory cytokines, such as IL-17A, which augment the migratory and invasive capabilities of tumor cells (37,38).

Concurrently, TAMs exhibit a distinct phenotypic polarization within lung metastases. In ccRCC pulmonary metastases, CD68/CD163 double-positive M2-like TAMs have been shown to densely infiltrate the tumor, often co-localizing with hypoxic niches marked by HIF-1α, and their presence has been linked to poor prognosis (9,39). By contrast, pulmonary metastases derived from prostate cancer have shown a notable enrichment of C-C chemokine receptor type 4 (CCR4)-positive myeloid cells, a recruitment pattern driven by the C-C motif chemokine ligand 22/CCR4 axis, which mirrors mechanisms observed in primary prostate tumors (40,41). The notable role of TAMs in fostering an immunosuppressive TME is underscored by intervention studies; depletion of TAMs using macrophage colony-stimulating factor 1 receptor (CSF-1R) inhibitors has been shown to repolarize remaining macrophages towards an antitumor M1 phenotype. This shift synergizes with agents such as sunitinib, leading to prolonged overall survival in preclinical models. As such, these findings highlight the central role of TAMs in fostering an immunosuppressive TME (39,42).

Immune checkpoints and spatial control of the T-cell response. The immune topography of metastases is characterized by the spatial segregation of cytotoxic lymphocytes. $CD8^+$ T cells are largely excluded from the tumor islets and confined to the invasive margins in a majority of pulmonary metastases (6,9,43). This exclusion pattern is associated with high expression levels of immune checkpoint ligands on the surrounding stromal cells, including CAFs and TAMs, rather than on the tumor cells themselves.

Among immune-evasion checkpoints, the programmed cell death protein 1 (PD-1)/PD-L1 axis remains the most extensively characterized. PD-L1 positivity has been detected in a notable proportion of pulmonary metastases derived from urological cancers, with observed frequencies aligning with their primary tumors (6,9). Notably, responses to immune-checkpoint blockade appear to be organ-specific. Pembrolizumab monotherapy has demonstrated a higher ORR in lung metastases derived from urothelial carcinoma at 38% compared with renal parenchymal lesions at 14%, implying that the pulmonary microenvironment may be intrinsically more permissive to T-cell-mediated cytotoxicity following checkpoint inhibition (6). Further analyses have revealed that lesions that respond to pembrolizumab often harbor tertiary lymphoid structures (TLSs), which are defined as organized clusters of immune cells in non-lymphoid tissues that serve as sites for local adaptive immune responses, and proliferating proliferation marker protein Ki-67^+ (Ki-67^+) PD-1^+ CD8 T cells; however, non-responding lesions are characterized by an IL-30^+ macrophage signature, which can be therapeutically targeted (6,10).

In addition to the PD-1/PD-L1 axis, other immune checkpoints, such as lymphocyte activation gene 3 protein (LAG-3) and T-cell immunoreceptor with Ig and ITIM domains (TIGIT), contribute to T-cell exhaustion. LAG-3 expression has been detected in tumor-infiltrating $CD4^+$ T cells in metastatic prostate cancer models (44). Fibrinogen-like protein 1 (FGL1), which is secreted by CAFs, has been identified as a major ligand for TIGIT in ccRCC and may contribute to TIGIT-mediated immune suppression (45). Preclinical evidence supports targeting these immune checkpoints; antibody-mediated neutralization of TIGIT has been shown to restore NK cell-mediated cytotoxicity and reduce pulmonary tumor burden, indicating the therapeutic potential of this strategy (46).

Therapeutic implications: Targeting the multicellular axis of the metastatic niche. The mechanistic interconnections between CAFs, TAMs and immune cells form a cycle of immune suppression within the established metastatic niche. This multicellular axis presents a compelling therapeutic opportunity to dismantle the tumor-supportive ecosystem rather than solely targeting the cancer cells themselves. The efficacy of this approach is predicated on simultaneously disrupting the pro-tumorigenic functions of multiple stromal components.

The targeting of CAFs has emerged as a viable strategy of compromising the structural integrity of the metastatic niche. Pharmacological inhibition of FAP-α, a key enzyme expressed by CAFs, has been shown to abrogate the pro-invasive effects of CAF-conditioned media (culture medium containing secreted factors from cancer-associated fibroblasts) on cancer cells, supporting FAP-α as a druggable target (37). CAF plasticity, defined as the capacity of CAFs to switch between pro-tumorigenic and anti-tumorigenic phenotypes as previously discussed in this section, suggests that targeting a single CAF-associated molecule may be insufficient. Therefore, the combination of FAP-targeted therapies with agents that block CAF-derived immunosuppressive cytokines represents a rational strategy to overcome phenotypic adaptation and prevent T-cell exclusion from the TME (31). Furthermore, neutralizing CAF-derived cytokines, such as IL-17A, has been shown to inhibit the pro-migratory signals that facilitate cancer-cell dissemination and tumoral niche maintenance (38).

Concurrently, reprogramming of the immune contexture by targeting TAMs has been shown to reverse immunosuppression. Therapeutic targeting of M2-like TAMs using CSF-1R inhibitors has been demonstrated to not only reduce the direct immunosuppressive influence of TAMs but also repolarize the macrophage population towards an immunostimulatory M1 phenotype (39,42). This shift has been demonstrated to synergize with anti-angiogenic agents, such as sunitinib, which can normalize the tumor vasculature by reversing abnormal vascular hyperpermeability and disorganized architecture that facilitate both tumor cell intravasation and extravasation, thereby improving T-cell infiltration and creating a more favorable microenvironment for immune attack (39,43).

Emerging clinical efforts are now formally testing the paradigm of stromal-immune axis disruption. These next-generation approaches refer to combination strategies designed to simultaneously target multiple cellular components of the TME, including CAFs and TAMs, to dismantle the physical and immunological barriers that protect metastatic lesions. Representative examples include trials combining CSF-1R inhibitors with PD-1/LAG-3 blockade, such as trial

NCT05577182, or FAP-α-targeted radioligands with IL-2, e.g. trial NCT06640413, which exemplify rational, next-generation approaches aimed at converting the pulmonary metastatic site from an immune sanctuary into a vulnerable target. Notably, the data from these ongoing trials remain preliminary, and their clinical utility requires future confirmation through expanded cohorts and validation in independent studies. The goal of these combinations is to dismantle the physical and biochemical barriers erected by the TME, thereby converting the pulmonary metastatic site from an immune sanctuary into a vulnerable target. This strategy, focused on targeting the 'soil' rather than just the 'seed', holds notable promise for improving outcomes in patients with metastatic disease spanning the lung-urological axis. However, the clinical translation of these microenvironmental insights is fundamentally predicated upon the accurate identification of the origin of tumors. As the molecular crosstalk and shared features of the TME in pulmonary and urological cancers frequently blur histological boundaries, distinguishing between primary lung neoplasms and urological metastases remains a notable clinical challenge. This challenge constitutes the first notable bottleneck in treating patients with pulmonary and urological cancer, necessitating the use of advanced diagnostic frameworks.

5. Diagnostic dilemmas and the path to precision

While molecular drivers and microenvironmental niches orchestrate the metastatic process, their clinical manifestation often presents as an ambiguous diagnostic landscape. Consequently, the management of metastatic cancer at the lung-urological interface is frequently complicated by notable diagnostic uncertainty. Accurately distinguishing a metastasis from a second primary tumor is not only an academic exercise but important in determining therapeutic strategies and prognosis. This section explores the clinical challenges and evolving role of advanced diagnostic modalities in identifying metastatic disease status, as well as the integrated approach required for precision medicine along the pulmonary-urological axis (Table III) (5,47-54).

Clinician's challenge: Distinguishing a metastasis from a second primary tumor. The initial clinical dilemma involved in distinguishing second primary tumors from metastases often arises from non-specific radiological findings. Solitary pulmonary nodules in a patient with a history of RCC or prostate cancer can represent either a metastatic deposit or a new primary lung adenocarcinoma. Conventional imaging modalities, such as computed tomography (CT), frequently lack the specificity required to differentiate between these entities, leading to diagnostic inertia and potential delays in initiating appropriate therapy. This challenge has been underscored by the results of clinicopathological analyses, which have revealed that a notable number of tumors at the pulmonary interface have been initially misclassified. For instance, a study has shown that solitary renal lesions in the context of a known lung primary tumor can be mistakenly diagnosed as second primaries, complicating cancer stage classification and treatment planning (47). The issue of tumor misclassification is further compounded by rare phenomena, such as tumor-to-tumor metastasis, and the existence of aggressive morphological variants, such as prostatic adenocarcinomas with urothelial-like features, which can blur histological boundaries and confound initial diagnostic efforts (49). Consequently, diagnostic reliance on patient clinical history and standard imaging alone is insufficient, necessitating the development of more sophisticated diagnostic algorithms.

Evolving role of pathology and molecular profiling. To resolve this diagnostic impasse, pathology has moved beyond traditional histology to incorporate sophisticated immunohistochemical panels and next-generation sequencing (NGS). IHC serves as the primary method for determining the tumoral tissue of origin (48). A panel including markers such as: i) PAX8 for detecting RCC; ii) TTF-1 for detecting lung adenocarcinoma; iii) GATA binding protein 3 to detect urothelial carcinoma; and iv) puromycin-sensitive aminopeptidase/P501S (prostein, a prostate-specific marker encoded by the SLC45A3 gene) for prostate cancer can provide decisive evidence in a number of cases (48). However, IHC has its limitations, particularly in poorly differentiated or rare tumor types. For example, RCCs exhibiting Xp11.2 translocation and *transcription factor E3* gene fusions exhibit a unique diagnostic profile that requires specific genetic or immunohistochemical confirmation beyond standard IHC markers (51). Similarly, the expression of cytokeratin (CK)7 and CK20 in some prostate cancers can mimic urothelial carcinoma, which highlights the potential for diagnostic misinterpretations using IHC and the need for a comprehensive marker panel (49).

In cases where IHC yields ambiguous or contradictory results, molecular profiling has emerged as a powerful adjunct. NGS can identify the lineage of a tumor by revealing pathognomonic genetic alterations (5). The analysis of metastatic patterns using ctDNA has proven particularly insightful. In a landmark study reported by Shiota *et al* (5), analysis of ctDNA from patients with castration-resistant prostate cancer demonstrated that the same AR-ligand binding-domain alteration present in the primary tumor was detectable in the majority of concurrent pulmonary metastases, whereas this modification was absent in synchronous primary lung cancers identified within the same cohort. This finding underscores the high specificity of clonal relatedness for confirming metastatic spread. Furthermore, NGS has revealed the genomic heterogeneity of metastases; for example, visceral metastases derived from prostate cancer often exhibit a distinct genomic landscape compared with bone metastases, with an enrichment of alterations in genes such as tumor protein p53 (TP53) and retinoblastoma-associated protein (RB1), as well as AR amplifications (52). This heterogeneity not only aids diagnosis, but also has profound implications for selecting targeted therapies; for example, the identification of specific MET mutations in papillary RCC may predict therapeutic responses to cabozantinib (50). The convergence of IHC and NGS thus provides a multi-modal diagnostic pathway, in which IHC offers a rapid, cost-effective method of initial tumor classification and NGS delivers definitive genomic evidence for challenging cases to guide therapeutic decision-making.

Promise of liquid biopsy and integrated diagnostic pathways. The advent of liquid biopsy represents a paradigm shift towards non-invasive, dynamic disease monitoring. Liquid

Table III. Diagnostic approach to metastatic tumors of uncertain origin at the lung-urological interface.

Clinical scenario	Recommended diagnostic algorithm	Key immunohistochemical markers	Value of molecular profiling or liquid biopsy	(Refs.)
Solitary pulmonary nodule in a patient with a history of RCC or prostate cancer	Clinical-radiological correlation followed by IHC, in turn followed by NGS if results are inconclusive.	For RCC metastasis vs. lung primary tumors: PAX8 positive and TTF-1 negative. For prostate metastasis vs. lung primary tumors: PSA/P501S positive and TTF-1 negative.	Confirms clonal origin; distinguishes metastasis from second primary.	(5,47,48)
Solitary renal lesion in a patient with a history of primary lung cancer	Clinical-radiological correlation followed by IHC, in turn followed by NGS if results are inconclusive.	For lung primary metastasis: TTF-1 positive and PAX8 negative. For challenging cases, including those with urothelial-like features or tumor-to-tumor metastasis, an extended panel incorporating CK7, CK20 or GATA3 may be required to resolve diagnostic ambiguity.	Identifies lineage-specific drivers; guides targeted therapy selection.	(47,49,50)
Poorly differentiated or rare tumor types, such as RCC with TFE3 gene fusions and urothelial-like prostate cancer	Comprehensive IHC followed by confirmatory genetic testing via FISH or NGS.	For RCC with TFE3 gene fusions: TFE3 shows strong nuclear positivity. Challenging cases may require extended panels, for example using IHC to detect CK7, CK20 or GATA3, to resolve ambiguity.	Definitive diagnosis via pathognomonic alterations.	(5,49,50)
Monitoring disease evolution and assessing tumor heterogeneity	Integration of radiological surveillance (e.g., computed tomography) and serial liquid biopsy via ctDNA analysis, as discussed in Section 5.	IHC is not the primary tool for dynamic monitoring	Tracks clonal evolution in real-time; assesses metastatic heterogeneity.	(52-54)

IHC, immunohistochemistry; NGS, next-generation sequencing; ctDNA, circulating tumor DNA; RCC, renal cell carcinoma; CK20, cytokeratin 20; GATA3, GATA binding protein 3; TFE3, transcription factor E3; CK7, cytokeratin 7; FISH, fluorescence *in situ* hybridization; PAX8, paired box 8; TTF-1, transcription termination factor 1; PSA, puromycin-sensitive aminopeptidase; P501S, prostein, a prostate-specific marker encoded by the *SLC45A3* gene.

biopsy is a non-invasive diagnostic modality that comprises the analysis of non-solid biological tissues, primarily blood, to detect tumor-derived genetic material, primarily through the analysis of ctDNA (55). A study reported by Esposito *et al* (55) demonstrated that monitoring tumor-derived cell-free DNA enables the non-invasive detection of genetic alterations in metastatic disease, offering clinical utility in early assessment of treatment response, real-time tracking of clonal evolution, and identification of resistance mechanisms without the need for repeat tissue biopsies. This promise has been cause for investigation, as ctDNA analysis allows for the genomic characterization of metastatic disease without the need for invasive tissue biopsy, which is particularly valuable in cases involving lesions that are difficult to access (53). For example, genomic amplifications identified in ctDNA, such as AR amplifications in metastatic castration-resistant prostate cancer (mCRPC), have provided both diagnostic confirmation of metastatic spread and important prognostic information (54).

Despite its promise as a diagnostic modality, the detection and molecular characterization of both CTCs and ctDNA has presented technical challenges in the clinical setting, including issues related to sensitivity and standardization (53). Notably, the clinical utility of liquid biopsy is severely constrained in low tumor-burden settings. In

scenarios involving solitary pulmonary nodules or early oligometastatic renal recurrences, the shedding of tumor DNA into the circulation is often insufficient to surpass the limit of detection of standard NGS assays. Consequently, a negative liquid biopsy result does not definitively exclude metastatic disease due to the risk of false negatives, necessitating a return to tissue sampling or close radiological surveillance in these indeterminate cases (53).

However, when successfully implemented, liquid biopsies can identify actionable alterations in tumor genomes and track clonal evolution in real time. This is especially relevant for predicting sites of metastasis; specific genomic signatures detected in ctDNA have been investigated as biomarkers for predicting the propensity of prostate cancer to metastasize to specific sites, such as bone or viscera (56). The integration of these biomarkers with traditional tissue-based diagnostics creates a powerful, complementary framework for accurate cancer diagnosis. This multi-step strategy aligns with contemporary diagnostic paradigms that advocate for the systematic integration of clinical, histopathological and molecular data to resolve diagnostic uncertainty in tumors of uncertain origin (48). This multi-step process ensures that patients receive a precise pathological assignment, following the recommended diagnostic algorithm outlined in Table III. As shown in Table III, this algorithm prioritizes the hierarchical application of IHC panels, for example PAX8 vs. TTF-1, to resolve common diagnostic ambiguities, whereas advanced molecular profiling is reserved for complex scenarios, such as solitary lesions with atypical morphology.

6. Therapeutic implications and the era of agnostic oncology

Building upon the aforementioned findings regarding the precise diagnostic stratification and elucidation of shared molecular drivers and immune contextures, the therapeutic landscape has been undergoing a notable transformation. The traditional paradigm of organ-specific therapy has been increasingly challenged by molecular evidence demonstrating that metastatic tumors derived from different primary tumors may share actionable genomic alterations (27,56,57). This convergence has catalyzed the emergence of agnostic oncology, which is also known as tissue-agnostic or tumor-agnostic therapy (27,57). This paradigm involves a shift in clinical decision-making, so that treatment is administered based on the presence of specific genomic alterations or molecular signatures, for example microsatellite instability-high (MSI-H) signatures, regardless of the histological origin or anatomical location of the tumor. In the specific context of lung-urological metastatic overlap, three therapeutic strategies exemplify this shift: i) Tissue-agnostic approval of ICIs for MSI-H or mismatch-repair deficient (dMMR) tumors; ii) targeted inhibition of shared oncogenic drivers, such as *neurotrophic receptor tyrosine kinase* fusions, *MET* exon 14 skipping or DNA-repair defects; and iii) targeting organ-specific differential responses to the same agent. These three strategies are outlined in Table IV (6,57-66), providing a structured framework for selecting the most appropriate mechanism-centric intervention based on the specific molecular profile of tumors.

From organ-centric to mechanism-centric therapy. Pembrolizumab was the first drug to receive tumor-agnostic approval by the Food and Drug Administration for use in targeting MSI-H or dMMR tumors (58). A 2023 real-world study of 3,112 ctDNA profiles revealed that MSI-H prevalence is comparable across pulmonary metastases of urothelial carcinoma and primary lung adenocarcinoma, which display prevalence rates of 6.8 and 5.9% respectively, supporting the cross-organ applicability of pembrolizumab in this molecular subset of tumors (58). Similarly, neurotrophic receptor tyrosine kinase (NTRK) fusion basket trials demonstrated an ORR >75% for larotrectinib regardless of primary tumor site; one of the 55 patients included in the study had a pulmonary metastasis from prostate cancer that achieved complete remission lasting 18 months (59). These findings validate the biological principle that a single type of genomic alteration can dominate metastatic behavior irrespective of organ ancestry.

Shared drivers in the lung-urological axis: MET, poly (ADP-ribose) polymerase (PARP) and beyond. MET exon 14 skipping occurs in 3-4% of patients with NSCLC and in ≤2% of papillary RCC. Savolitinib, a selective MET inhibitor, produced a 42% partial-response rate among 26 patients with papillary RCC and lung-dominant metastatic disease (60), mirroring the 44% ORR reported in patients with NSCLC harboring the same alteration. This comparable efficacy across distinct tumor types harboring the same molecular alteration supports true clonal sensitivity rather than organ-specific pharmacokinetic activity.

PARP inhibition represents another mechanism-centric therapeutic strategy. In the TALAPRO-1 trial (ClinicalTrials.gov identifier: NCT03148795), talazoparib monotherapy yielded a 46% ORR in mCRPC that exhibited DNA-repair defects; notably, targeted lung lesions shrank in 9 of 11 cases, whereas bone lesions responded in only 18%, suggesting organ-specific modulation of drug efficacy (61). The subsequent JAVELIN PARP Medley trial (ClinicalTrials.gov identifier: NCT03330405) extended this concept to solid non-prostate tumors: Administration of avelumab combined with talazoparib achieved a 30% ORR in MSI-H or ataxia telangiectasia mutated (ATM)-deficient tumors, including in 2 patients with urothelial carcinoma that exhibited lung metastases that had progressed after platinum-based chemotherapy (62). Collectively, these observations indicated that homologous recombination deficiency (HRD), including deficiency in ATM and other DNA repair genes, is a trans-organ predictive biomarker of therapeutic efficacy, but that the metastatic-site microenvironment may still influence the depth and durability of therapeutic responses.

ICIs: Organ-specific efficacy within an agnostic frame. Despite the agnostic approval of pembrolizumab for MSI-H tumors, organ-specific response patterns have been increasingly reported. A study by Furubayashi *et al* (6) retrospectively compared pulmonary vs. renal-parenchymal lesions in 92 patients with urothelial carcinoma receiving pembrolizumab after platinum failure who were not preselected based on microsatellite instability-high (MSI-H) status (i.e., an all-comer population); the ORR of lung metastases was 38%, which was identical to lymph-node disease, whereas the ORR

Table IV. Therapeutic paradigms in the lung-urological metastatic axis.

Therapeutic domain	Molecular target or biomarker	Key agents	Evidence in the lung-urological axis	(Refs.)
Tissue-agnostic therapy	MSI-H or dMMR; NTRK fusions	Pembrolizumab and larotrectinib	Comparable MSI-H prevalence in lung and urothelial cancer metastases; efficacy of larotrectinib in prostate cancer pulmonary metastasis.	(58,59)
Shared oncogenic drivers	*MET* exon 14 skipping	Savolitinib	Similar response rates in papillary RCC with lung metastases and primary NSCLC harboring MET alterations.	(60)
Shared DNA-repair defects	HRD, for example BRCA or ATM	Talazoparib; talazoparib + avelumab	High response in lung lesions of mCRPC; activity in MSI-H- or ATM-deficient urothelial carcinoma with lung metastases.	(61,62)
Organ-specific efficacy of ICIs (combination)	PD-1/PD-L1	Nivolumab + ipilimumab	Cases of pulmonary remission with concurrent bone progression in RCC.	(63)
Organ-specific efficacy of ICIs (combination)	PD-1/PD-L1	Pembrolizumab; nivolumab	Higher ORR in lung vs. renal parenchymal metastases from UC.	(6,64)
Complex predictive biomarkers	TMB; tryptophan catabolism	N/A	Differential predictive power of TMB cut-offs in lung vs. urothelial cancers; association of elevated IDO activity with lung-targeted immunotherapy resistance.	(57,65,66)

MSI-H, microsatellite instability-high; dMMR, mismatch-repair deficient; HRD, homologous recombination deficiency; mCRPC, metastatic castration-resistant prostate cancer; ICIs, immune-checkpoint inhibitors; UC, urothelial carcinoma; RCC, renal cell carcinoma; ORR, objective response rate; TMB, tumor mutational burden; PD-1, programmed cell death protein 1; PD-L1, programmed death-ligand 1; IDO, indoleamine 2,3-dioxygenase; ATM, ataxia telangiectasia mutated; BRCA, breast cancer susceptibility protein; NSCLC, non-small cell lung cancer; MET, mesenchymal-epithelial transition; NTRK, neurotrophic receptor tyrosine kinase; N/A, not applicable.

of renal parenchymal metastases was only 14%. Multiplex immunofluorescence revealed that responding lung lesions were enriched in TLSs and Ki-67$^+$ PD-1$^+$ CD8$^+$ T cells, whereas non-responding renal lesions harbored an IL-30$^+$ macrophage signature, implying that myeloid exclusion networks may counteract T-cell reinvigoration in specific metastatic niches (6).

These findings are consistent with case-level observations in RCC; two independent reports have documented complete pulmonary remission following nivolumab monotherapy or combination treatments with nivolumab and ipilimumab, whereas concurrent bone lesions progressed (6,63). Conversely, hyperprogression in pulmonary metastases has also been described following treatment with ICIs. A 2021 case report highlighted the notable growth of lung lesions in a patient with metastatic RCC receiving radiotherapy and anti-PD-1 therapy; however, extra-pulmonary metastatic sites remained stable, underscoring the dual capacity of the pulmonary microenvironment to either amplify or attenuate ICI activity (64). However, caution is warranted in attributing these response patterns solely to microenvironmental distinctiveness. Confounding variables, including the immunosuppressive sequelae of prior systemic therapies and the inherent genomic heterogeneity of metastatic subclones, may also contribute to these site-dependent discrepancies in treatment efficacy, as evidenced by the distinct mutational landscapes observed between visceral and bone metastases (52).

Biomarker complexity: Tumor mutational burden (TMB), PD-L1 and beyond. TMB has gained traction as a pan-cancer biomarker, yet threshold validity values differ between pulmonary and urological metastases. A study reported by Passaro *et al* (65) noted that a TMB≥10 mutations/Mb predicted therapeutic benefits of ICI treatment in NSCLC with a positive predictive value (PPV) of 68%, whereas the same cutoff in urothelial carcinoma yielded a PPV of only 45%. ctDNA analyses have further revealed that sub-clonal TMB, rather than bulk TMB, associates with pulmonary metastatic relapse after ICI discontinuation, suggesting that spatial heterogeneity may obscure binary TMB cutoffs (66). Tryptophan catabolism, which is measured by determining the plasma kynurenine/tryptophan ratio, has also emerged as an orthogonal resistance mechanism. A study reported by Botticelli *et al* (57) demonstrated that the level of indoleamine 2,3-dioxygenase 1 activity in patients with progressive disease involving lung metastases was three-fold higher than that observed in patients with progressive disease involving lymph nodes during pembrolizumab therapy, indicating that metabolic immune escape may be particularly active in pulmonary niches.

7. Future perspectives

The increasing recognition of the lung-urological metastatic overlap has necessitated a shift from reactive tumor management to proactive, mechanism-based strategies (20,27,57). Although the integration of multidisciplinary teams (MDTs), defined as collaborative groups of healthcare professionals from diverse specialties such as urology, thoracic surgery, medical oncology, radiology and pathology, and advanced sequencing platforms constitutes the immediate next step for advancing treatments targeting tumors along this axis, the long-term goal remains the translation of molecular discoveries into tangible clinical benefits. Specifically, translational efforts should prioritize the pharmacological disruption of the CXCR4/CXCL12 axis, for example by using repurposed antagonists such as plerixafor, to block metastatic seeding, as well as the standardization of detecting exosomal miR-210-3p as a non-invasive biomarker for early intervention. Ultimately, future management of the lung-urological metastatic overlap necessitates a dual approach aimed at simultaneously refining diagnostic precision through agnostic oncology frameworks and enhancing therapeutic specificity by translating molecular insights into targeted interventions for investigation in prospective clinical trials.

Liquid biopsy-mediated analysis of ctDNA in particular represents a cornerstone diagnostic modality for the dynamic monitoring of pulmonary and urological tumors in the future. A prospective study has provided evidence that rising ctDNA levels can predict radiographic progression in pulmonary metastases from prostate cancer or RCC weeks in advance (67). However, the analytical sensitivity of ctDNA assays does not remain uniform across metastatic sites. Recent high-impact research reported by Afridi *et al* (68) highlighted a notable limitation of ctDNA analysis: Standard mutant allele fraction thresholds that are sensitive for lung-target lesions often fail to detect bone metastases. This finding underscores the necessity of adaptive, organ-specific ctDNA thresholds that integrate both tumor burden and metastatic location to avoid false-negative stratification. While technological refinements, such as duplex sequencing, can enhance ctDNA sensitivity across anatomical sites, these often increase costs and may still fail in cases involving exceedingly low CTC counts (67). Therefore, the future clinical utility of ctDNA analysis will depend on standardized, cost-effective assays validated in large-scale intervention trials to confirm that pre-emptive treatment modification guided by molecular relapse (defined as a sustained increase in ctDNA levels indicating impending radiographic progression before overt clinical or imaging evidence of disease) improves survival outcomes.

Concurrently, the integration of artificial intelligence (AI) with medical imaging has unlocked novel diagnostic and predictive capabilities. Radiomic signatures extracted from CT scans based on AI algorithms can non-invasively predict molecular features, such as EGFR mutation status in brain metastases of lung adenocarcinoma (69). Furthermore, a study reported by Leivaditis *et al* (70) emphasized that AI surpassed its use in simple diagnostics to become an integral part of thoracic surgical planning. The analysis in the aforementioned study demonstrated that AI-driven models can now predict perioperative risks and long-term survival in complex metastatic resections, advocating for the inclusion of AI metrics in MDT decision-making processes. Despite this promise, vendor dependency and a lack of standardization in AI model training across different cohorts and imaging platforms remain major obstacles to the widespread clinical deployment of AI; external validation studies often report diminished performance levels when AI algorithms are applied to images acquired from different CT scanner models from those they are trained on (71,72). Federated learning platforms, which enable the pooling of imaging, genomic and clinical data across institutions without compromising patient privacy and are currently piloted by international consortia, represent a promising next step for overcoming cohort heterogeneity and building robust, generalizable models (73).

Regarding tissue diagnostics, spatial transcriptomics and multiplex immunoprofiling have revealed the profound impact of the spatial architecture of the TME on therapeutic responses. These technologies have consistently shown that TLSs are enriched in pulmonary metastases and associate with promising responses to immune-checkpoint blockade independently of traditional biomarkers, such as tumor mutational burden (74). Conversely, TLS are virtually absent in paired renal parenchymal metastases, highlighting the fundamental, organ-specific differences in immune topography that influence treatment efficacy (74,75). The translation of these insights will involve developing spatial theranostics, which are diagnostic tests that can guide targeted therapies based on the spatial context of the TME. For example, FAP-targeted PET tracers have achieved high tumor-to-background signal ratios in both primary lung tumors and pulmonary metastases derived from urological primaries, providing pan-cancer read-outs of the metastatic niche (76). However, dosimetry modeling has revealed high renal cortex uptake of these tracers, raising nephrotoxicity concerns for subsequent FAP-directed radionuclide therapies and necessitating thorough risk-benefit assessments (76). Similarly, CXCR4-directed PET has demonstrated heterogeneous intra-pulmonary tracer distribution, with hotspots co-localizing with immune-suppressive, $CD163^{+}$ macrophage-rich regions, suggesting that future radiotherapeutic strategies may require 'dose painting' to effectively target these immune-excluded sub-niches (77,78).

Therapeutic innovation has become increasingly focused on targeting the metastatic organ itself, leading to the development of designer nanotherapies and cell-based products. A breakthrough study in Molecular Cancer has advanced this therapeutic innovation by developing nanoparticle-formulated chimeric antigen receptor T-cell (CAR-T) therapies. The study demonstrated that these nanocarriers markedly enhanced the accumulation of therapeutic agents within pulmonary metastases when compared with normal drug administration and concurrently reduced systemic toxicity (79). Notably, the enhancement of drug accumulation observed in lung tumors was equivalent for metastases originating from both prostate and renal primary tumors. This implied that organ-specific vascular permeability, rather than cancer histology, is a key determinant of pharmacokinetics (79). In terms of cellular therapy, CAR-Ts engineered to secrete anti-PD-L1 nanobodies have been shown to proliferate robustly within pulmonary lesions but exhibit poor persistence in renal parenchymal

tumors. This disparity reflects the underlying site-specific immune landscapes, wherein pulmonary metastases are characterized by an immune-excluded phenotype with CD8+ T cells confined to the invasive margins, as detailed in section 4 of this review (80). The robust proliferation of engineered CAR-T cells within these pulmonary lesions highlights a therapeutic strategy designed to overcome, rather than contradict, this native immune barrier. These findings collectively support the utility of advanced therapies in which the homing moieties, payload release kinetics and co-stimulatory domains (e.g., CD28 or 4-1BB signaling modules that enhance T-cell activation and persistence) are tailored to the unique biology of the metastatic organ.

Deciphering the lung-urological metastatic axis requires the evolution of anticancer therapeutic strategies from systemic therapies to precision medicine. The integration of AI-driven predictive modeling and organotropic nanotherapies remains a priority for translational cancer research. Future efforts should focus on validating these modalities in clinical trials to address microenvironmental heterogeneity. Ultimately, disruption of the molecular crosstalk within the lung-urological metastatic axis holds the potential to redefine standards of care and improve survival outcomes for patients exhibiting this complex metastatic disease.

8. Conclusions

Elucidation of the metastatic overlap between pulmonary and urological malignancies requires a fundamental paradigm shift. Notably, the synthesis of previous data highlights two major breakthroughs. Primarily, the identification of common targets of cross-organ metastasis offers a biological rationale for deploying tissue-agnostic therapies. Furthermore, tumor-mediated regulation of the organ microenvironment acts as a decisive determinant of clinical outcomes and therapeutic responses. As such, integrating these shared molecular vulnerabilities with niche-specific observations remains important for improving patient survival in this complex patient cohort.

Acknowledgements

Not applicable.

Funding

No funding was received.

Availability of data and materials

Not applicable.

Authors' contributions

YW conducted the literature search, drafted the original manuscript and prepared the figures and tables. JG conceived the focus of the review, supervised the overall project and critically revised and edited the manuscript for intellectual content. All authors read and approved the final manuscript. Data authentication is not applicable.

Ethics approval and consent to participate

Not applicable.

Patient consent for publication

Not applicable.

Competing interests

The authors declare that they have no competing interests.

References

1. Deng Y, Bi R, Zhu Z, Li S, Xu B, Rather WA and Wang C: A surveillance, epidemiology and end results database analysis of the prognostic value of organ-specific metastases in patients with advanced prostatic adenocarcinoma. Oncol Lett 18: 1057-1070, 2019.
2. Surveillance, Epidemiology, and End Results (SEER) Program. SEER*Stat Database: Incidence-SEER Research Data, 8 Registries, Nov 2024 Sub (1975-2022). National Cancer Institute, Division of Cancer Control and Population Sciences, Surveillance Research Program. Released April 2025. Available from: www.seer.cancer.gov.
3. Epstein JI, Egevad L, Amin MB, Delahunt B, Srigley JR and Humphrey PA; Grading Committee: The 2014 International society of urological pathology (ISUP) consensus conference on Gleason grading of prostatic carcinoma: Definition of grading patterns and proposal for a new grading system. Am J Surg Pathol 40: 244-252, 2016.
4. Wei H, Miao J, Cui J, Zheng W, Chen X, Zhang Q, Liu F, Mao Z, Qiu S and Zhang D: The prognosis and clinicopathological features of different distant metastases patterns in renal cell carcinoma: Analysis based on the SEER database. Sci Rep 11: 17822, 2021.
5. Shiota M, Matsubara N, Kato T, Eto M, Osawa T, Abe T, Shinohara N, Nishimoto K, Yasumizu Y, Tanaka N, *et al*: Genomic characterization of metastatic patterns in prostate cancer using circulating tumor DNA data from the SCRUM-Japan MONSTAR SCREEN project. J Liq Biopsy 7: 100282, 2024.
6. Furubayashi N, Negishi T, Sakamoto N, Shimokawa H, Morokuma F, Song Y, Hori Y, Tomoda T, Tokuda N, Seki N, *et al*: Organ-specific tumor response to pembrolizumab in advanced urothelial carcinoma after Platinum-based chemotherapy. Onco Targets Ther 14: 1981-1988, 2021.
7. Zhuang W, Li Y, Chen P, Wang J, Liu W and Chen J: Do renal cell carcinoma patients with brain metastases still need nephrectomy? Int Urol Nephrol 51: 941-949, 2019.
8. Hamadi R, Karam I, Khan S, Homsy S and Luhrs C: Tumour-To-Tumour metastasis: A rare case of prostate cancer metastasising to primary lung adenocarcinoma. Eur J Case Rep Intern Med 11: 004579, 2024.
9. Steindl A, Alpar D, Heller G, Mair MJ, Gatterbauer B, Dieckmann K, Widhalm G, Hainfellner JA, Schmidinger M, Bock C, *et al*: Tumor mutational burden and immune infiltrates in renal cell carcinoma and matched brain metastases. ESMO Open 6: 100057, 2021.
10. Sorrentino C, Yin Z, Ciummo S, Lanuti P, Lu LF, Marchisio M, Bellone M and Di Carlo E: Targeting Interleukin(IL)-30/IL-27p28 signaling in cancer stem-like cells and host environment synergistically inhibits prostate cancer growth and improves survival. J Immunother Cancer 7: 201, 2019.
11. Hakozaki K, Tanaka N, Takamatsu K, Takahashi R, Yasumizu Y, Mikami S, Shinojima T, Kakimi K, Kamatani T, Miya F, *et al*: Landscape of prognostic signatures and immunogenomics of the AXL/GAS6 axis in renal cell carcinoma. Br J Cancer 125: 1533-1543, 2021.
12. Chen J, Cao N, Li S and Wang Y: Identification of a risk stratification model to predict overall survival and surgical benefit in clear cell renal cell carcinoma with distant metastasis. Front Oncol 11: 630842, 2021.
13. Wang L, Yang G, Zhao D, Wang J, Bai Y, Peng Q, Wang H, Fang R, Chen G, Wang Z, *et al*: CD103-positive CSC exosome promotes EMT of clear cell renal cell carcinoma: Role of remote MiR-19b-3p. Mol Cancer 18: 86, 2019.

14. Petrozza V, Costantini M, Tito C, Giammusso LM, Sorrentino V, Cacciotti J, Porta N, Iaiza A, Pastore AL, Di Carlo A, *et al*: Emerging role of secreted miR-210-3p as potential biomarker for clear cell renal cell carcinoma metastasis. Cancer Biomark 27: 181-188, 2020.
15. Cai Q, Chen Y, Zhang D, Pan J, Xie Z, Ma S, Liu C, Zuo J, Zhou X, Quan C, *et al*: Loss of epithelial AR increase castration resistant stem-like prostate cancer cells and promotes cancer metastasis via TGF-β1/EMT pathway. Transl Androl Urol 9: 1013-1027, 2020.
16. Li W, Yang FQ, Sun CM, Huang JH, Zhang HM, Li X, Wang GC, Zhang N, Che JP, Zhang WT, *et al*: circPRRC2A promotes angiogenesis and metastasis through epithelial-mesenchymal transition and upregulates TRPM3 in renal cell carcinoma. Theranostics 10: 4395-4409, 2020.
17. Wu N, Wang Y, Wang K, Zhong B, Liao Y, Liang J and Jiang N: Cathepsin K regulates the tumor growth and metastasis by IL-17/CTSK/EMT axis and mediates M2 macrophage polarization in castration-resistant prostate cancer. Cell Death Dis 13: 813, 2022.
18. Chen X, Jia Y, Zhang Y, Zhou D, Sun H and Ma X: α5-nAChR contributes to epithelial-mesenchymal transition and metastasis by regulating Jab1/Csn5 signalling in lung cancer. J Cell Mol Med 24: 2497-2506, 2020.
19. Cao Q, Liu Y, Wu Y, Hu C, Sun L, Wang J, Li C, Guo M, Liu X, Lv J, *et al*: Profilin 2 promotes growth, metastasis, and angiogenesis of small cell lung cancer through cancer-derived exosomes. Aging (Albany NY) 12: 25981-25999, 2020.
20. Davoodvandi A, Darvish M, Borran S, Nejati M, Mazaheri S, Reza Tamtaji O, Hamblin MR, Masoudian N and Mirzaei H: The therapeutic potential of resveratrol in a mouse model of melanoma lung metastasis. Int Immunopharmacol 88: 106905, 2020.
21. Masuda C, Sugimoto M, Wakita D, Monnai M, Ishimaru C, Nakamura R, Kinoshita M, Yorozu K, Kurasawa M, Kondoh O and Yamamoto K: Bevacizumab suppresses the growth of established non-small-cell lung cancer brain metastases in a hematogenous brain metastasis model. Clin Exp Metastasis 37: 199-207, 2020.
22. Berta J, Török S, Tárnoki-Zách J, Drozdovszky O, Tóvári J, Paku S, Kovács I, Czirók A, Masri B, Megyesfalvi Z, *et al*: Apelin promotes blood and lymph vessel formation and the growth of melanoma lung metastasis. Sci Rep 11: 5798, 2021.
23. Wang B, Pan LY, Kang N and Shen XY: PP4R1 interacts with HMGA2 to promote non-small-cell lung cancer migration and metastasis via activating MAPK/ERK-induced epithelial-mesenchymal transition. Mol Carcinog 59: 467-477, 2020.
24. Zhang B, Li Y, Wu Q, Xie L, Barwick B, Fu C, Li X, Wu D, Xia S, Chen J, *et al*: Acetylation of KLF5 maintains EMT and tumorigenicity to cause chemoresistant bone metastasis in prostate cancer. Nat Commun 12: 1714, 2021.
25. Shin SB, Jang HR, Xu R, Won JY and Yim H: Active PLK1-driven metastasis is amplified by TGF-β signaling that forms a positive feedback loop in non-small cell lung cancer. Oncogene 39: 767-785, 2020.
26. Gallazzi M, Baci D, Mortara L, Bosi A, Buono G, Naselli A, Guarneri A, Dehò F, Capogrosso P, Albini A, *et al*: Prostate cancer peripheral blood NK cells show enhanced CD9, CD49a, CXCR4, CXCL8, MMP-9 production and secrete monocyte-recruiting and polarizing factors. Front Immunol 11: 586126, 2020.
27. Li L, Zhao L, Yang J and Zhou L: Multifaceted effects of LRP6 in cancer: Exploring tumor development, immune modulation and targeted therapies. Med Oncol 41: 180, 2024.
28. Ruan T, Jiang L, Xu J and Zhou J: Abiraterone suppresses irradiated lung cancer cells-induced angiogenic capacities of endothelial cells. J Bioenerg Biomembr 53: 343-349, 2021.
29. Chang YC, Liu CT, Yu CY and Sung WW: NPS-1034 exerts therapeutic efficacy in renal cell carcinoma through multiple targets of MET, AXL, and TNFRSF1A signaling in a metastatic model. Cells 13: 1713, 2024.
30. Greifenstein L, Kramer CS, Moon ES, Rösch F, Klega A, Landvogt C, Müller C and Baum RP: From automated synthesis to in vivo application in multiple types of Cancer-clinical results with [68Ga]Ga-DATA5m.SA.FAPi. Pharmaceuticals (Basel) 15: 1000, 2022.
31. Kraxner A, Braun F, Cheng WY, Yang TO, Pipaliya S, Canamero M, Andersson E, Harring SV, Dziadek S, Bröske AE, *et al*: Investigating the complex interplay between fibroblast activation protein α-positive cancer associated fibroblasts and the tumor microenvironment in the context of cancer immunotherapy. Front Immunol 15: 1352632, 2024.
32. Yu W, Zhang X, Zhang W, Xiong M, Lin Y, Chang M, Xu L, Lu Y, Liu Y and Zhang J: 19-Hydroxybufalin inhibits non-small cell lung cancer cell proliferation and promotes cell apoptosis via the Wnt/β-catenin pathway. Exp Hematol Oncol 10: 48, 2021.
33. Watts A, Singh B, Singh H, Kaur H, Bal A, Vohra M, Arora SK and Behera D: 68Ga-pentixafor PET/CT demonstrating in vivo CXCR4 receptor overexpression in rare lung malignancies: Correlation with histologic and histochemical findings. J Nucl Med Technol 50: 278-281, 2022.
34. Slania SL, Das D, Lisok A, Du Y, Jiang Z, Mease RC, Rowe SP, Nimmagadda S, Yang X, Pomper MG, *et al*: Imaging of fibroblast activation protein in cancer xenografts using novel (4-Quinolinoyl)-glycyl-2-cyanopyrrolidine-Based small molecules. J Med Chem 64: 4059-4070, 2021.
35. Manawy SM, Faruk EM, Hindawy RF, Hassan MM, Farrag DMG, Bashar MAE, Fouad H, Bagabir RA, Hassan DAA, Zaazaa AM, *et al*: Modulation of the Sirtuin-1 signaling pathway in doxorubicin-induced nephrotoxicity (synergistic amelioration by resveratrol and pirfenidone). Tissue Cell 87: 102330, 2024.
36. Zheng Y, Yang S, Si J, Zhao Y, Zhao M and Ji E: Shashen-maidong decoction inhibited cancer growth under intermittent hypoxia conditions by suppressing oxidative stress and inflammation. J Ethnopharmacol 299: 115654, 2022.
37. Liu X, Tang J, Peng L, Nie H, Zhang Y and Liu P: Cancer-associated fibroblasts promote malignant phenotypes of prostate cancer cells via autophagy: Cancer-associated fibroblasts promote prostate cancer developmentt. Apoptosis 28: 881-891, 2023.
38. Gao F, Chen X, Li X, Deng C and Luo P: The Pro-migratory and Pro-invasive roles of cancer-associated fibroblasts secreted IL-17A in prostate cancer. J Biochem Mol Toxicol 39: e70047, 2025.
39. Li H, Ding J, Lu M, Liu H, Miao Y, Li L, Wang G, Zheng J, Pei D and Zhang Q: CAIX-specific CAR-T cells and sunitinib show synergistic effects against metastatic renal cancer models. J Immunother 43: 16-28, 2020.
40. Maolake A, Izumi K, Shigehara K, Natsagdorj A, Iwamoto H, Kadomoto S, Takezawa Y, Machioka K, Narimoto K, Namiki M, *et al*: Tumor-associated macrophages promote prostate cancer migration through activation of the CCL22-CCR4 axis. Oncotarget 8: 9739-9751, 2017.
41. Shi F, Sun MH, Zhou Z, Wu L, Zhu Z, Xia SJ, Han BM, Zhao YY, Jing YF and Cui D: Tumor-associated macrophages in direct contact with prostate cancer cells promote malignant proliferation and metastasis through NOTCH1 pathway. Int J Biol Sci 18: 5994-6007, 2022.
42. Wang C, Wang Y, Hong T, Ye J, Chu C, Zuo L, Zhang J and Cui X: Targeting a positive regulatory loop in the tumor-macrophage interaction impairs the progression of clear cell renal cell carcinoma. Cell Death Differ 28: 932-951, 2021.
43. O'Shaughnessy MJ, Murray KS, La Rosa SP, Budhu S, Merghoub T, Somma A, Monette S, Kim K, Corradi RB, Scherz A and Coleman JA: Systemic antitumor immunity by PD-1/PD-L1 Inhibition is potentiated by Vascular-targeted photodynamic therapy of primary tumors. Clin Cancer Res 24: 592-599, 2018.
44. Zhao Y, Peng X, Baldwin H, Zhang C, Liu Z and Lu X: Anti-androgen therapy induces transcriptomic reprogramming in metastatic castration-resistant prostate cancer in a murine model. Biochim Biophys Acta Mol Basis Dis 1867: 166151, 2021
45. Lv Z, Cui B, Huang X, Feng HY, Wang T, Wang HF, Xuan YD, Li HZ, Ma X, Huang Y and Zhang X: FGL1 as a novel mediator and biomarker of malignant progression in clear cell renal cell carcinoma. Front Oncol 11: 756843, 2021.
46. Zhang Y, Wang X, Gu Y, Liu T, Zhao X, Cheng S, Duan L, Huang C, Wu S and Gao S: Complement C3 of tumor-derived extracellular vesicles promotes metastasis of RCC via recruitment of immunosuppressive myeloid cells. Proc Natl Acad Sci USA 122: e2420005122, 2025.
47. Zhu Y, Han CH, Yang YL, Xu JJ and Yu YW: Metastatic renal cell carcinoma: A clinicopathological analysis of 196 cases. Zhonghua Bing Li Xue Za Zhi 49: 1255-1260, 2020 (In Chinese).
48. Herrington CS, Poulsom R and Coates PJ: Recent advances in pathology: The 2019 annual review issue of the journal of pathology. J Pathol 247: 535-538, 2019.
49. Nguyen NJ, Sherman C, van der Kwast TH and Downes MR: Aggressive prostatic adenocarcinoma with urothelial-like morphology, with frequent CK7/CK20/HMWK expression and occasional diffuse neuroendocrine features: A clinicopathologic study of 12 cases. Pathol Res Pract 254: 155105, 2024.

50. Zhao H, Nolley R, Chan AMW, Rankin EB and Peehl DM: Cabozantinib inhibits tumor growth and metastasis of a patient-derived xenograft model of papillary renal cell carcinoma with MET mutation. Cancer Biol Ther 18: 863-871, 2017.
51. Yu W, Wang Y, Rao Q, Jiang Y, Zhang W and Li Y: Xp11.2 translocation renal neoplasm with features of TFE3 rearrangement associated renal cell carcinoma and Xp11 translocation renal mesenchymal tumor with melanocytic differentiation harboring NONO-TFE3 fusion gene. Pathol Res Pract 215: 152521, 2019.
52. Gong Y, Fan L, Fei X, Zhu Y, Du X, He Y, Pan J, Dong B and Xue W: Targeted Next-generation sequencing reveals heterogenous genomic features in viscerally metastatic prostate cancer. J Urol 206: 279-288, 2021.
53. Strati A, Markou A, Kyriakopoulou E and Lianidou E: Detection and molecular characterization of circulating tumour cells: Challenges for the clinical setting. Cancers (Basel) 15: 2185, 2023.
54. Dincman TA, Karam JAQ, Giordano A, Li H, Drusbosky LM, Gourdin TS, Howe PH and Lilly MB: Genomic amplifications identified by circulating tumor DNA analysis guide prognosis in metastatic castration-resistant prostate cancer. Front Oncol 13: 1202277, 2023.
55. Esposito A, Bardelli A, Criscitiello C, Colombo N, Gelao L, Fumagalli L, Minchella I, Locatelli M, Goldhirsch A and Curigliano G: Monitoring tumor-derived cell-free DNA in patients with solid tumors: Clinical perspectives and research opportunities. Cancer Treat Rev 40: 648-655, 2014.
56. Ying M, Mao J, Sheng L, Wu H, Bai G, Zhong Z and Pan Z: Biomarkers for prostate cancer bone metastasis detection and prediction. J Pers Med 13: 705, 2023.
57. Botticelli A, Mezi S, Pomati G, Cerbelli B, Cerbelli E, Roberto M, Giusti R, Cortellini A, Lionetto L, Scagnoli S, *et al*: Tryptophan catabolism as immune mechanism of primary resistance to Anti-PD-1. Front Immunol 11: 1243, 2020.
58. Kasi PM, Bucheit LA, Liao J, Starr J, Barata P, Klempner SJ, Gandara D, Shergill A, Madeira da Silva L, Weipert C, *et al*: Pan-cancer prevalence of microsatellite Instability-High (MSI-H) identified by circulating tumor DNA and Associated Real-world clinical outcomes. JCO Precis Oncol 7: e2300118, 2023.
59. Pollack M, Keating K, Wissinger E, Jackson L, Sarnes E and Cuffel B: Transforming approaches to treating TRK fusion cancer: Historical comparison of larotrectinib and histology-specific therapies. Curr Med Res Opin 37: 59-70, 2021.
60. Markham A: Savolitinib: First approval. Drugs 81: 1665-1670, 2021.
61. de Bono JS, Mehra N, Scagliotti GV, Castro E, Dorff T, Stirling A, Stenzl A, Fleming MT, Higano CS, Saad F, *et al*: Talazoparib monotherapy in metastatic Castration-resistant prostate cancer with DNA repair alterations (TALAPRO-1): An open-label, phase 2 trial. Lancet Oncol 22: 1250-1264, 2021.
62. Yap TA, Bardia A, Dvorkin M, Galsky MD, Beck JT, Wise DR, Karyakin O, Rubovszky G, Kislov N, Rohrberg K, *et al*: Avelumab plus talazoparib in patients with advanced solid tumors: The JAVELIN PARP medley nonrandomized controlled trial. JAMA Oncol 9: 40-50, 2023.
63. Danno T, Iwata S, Niimi F, Honda S, Okada H and Azuma T: Nivolumab and ipilimumab combination immunotherapy for patients with metastatic collecting duct carcinoma. Case Rep Urol 2021: 9936330, 2021.
64. Liu C, Piao J and Shang Z: Hyperprogressive disease after radiotherapy combined with anti-PD-1 therapy in renal cell carcinoma: A case report and review of the literature. BMC Urol 21: 42, 2021.
65. Passaro A, Stenzinger A and Peters S: Tumor mutational burden as a Pan-cancer biomarker for immunotherapy: The limits and potential for convergence. Cancer Cell 38: 624-625, 2020.
66. Chen A, Zhang S, Xiong L, Xi S, Tao R, Chen C, Li J, Chen J and Li C: Investigation of an Alternative marker for hypermutability evaluation in different tumors. Genes (Basel) 12: 197, 2021.
67. Zhang C, Liu Y, Chen Z, Liu YI, Mao Q, Zhang GE, Lin H, Zheng J and Li H: Current status, hotspots, and trends in cancer prevention, screening, diagnosis, treatment, and rehabilitation: A bibliometric analysis. Oncol Res 33: 1437-1458, 2025.
68. Afridi WA, Picos SH, Bark JM, Stamoudis DAF, Vasani S, Irwin D, Fielding D and Punyadeera C: Minimally invasive biomarkers for triaging lung nodules-challenges and future perspectives. Cancer Metastasis Rev 44: 29, 2025.
69. Tabnak P, Kargar Z, Ebrahimnezhad M and HajiEsmailPoor Z: A Bayesian meta-analysis on MRI-based radiomics for predicting EGFR mutation in brain metastasis of lung cancer. BMC Med Imaging 25: 44, 2025.
70. Leivaditis V, Maniatopoulos AA, Lausberg H, Mulita F, Papatriantafyllou A, Liolis E, Beltsios E, Adamou A, Kontodimopoulos N and Dahm M: Artificial intelligence in thoracic surgery: A review bridging innovation and clinical practice for the next generation of surgical care. J Clin Med 14: 2729, 2025.
71. Tang F, Zha XK, Ye W, Wang YM, Wu YF, Wang LN, Lyu LP and Lyu XM: Artificial intelligence-assisted endobronchial ultrasound for differentiating between benign and malignant thoracic lymph nodes: A meta-analysis. BMC Pulm Med 25: 303, 2025.
72. Zhang L, Yang D, Ye X and Bai C: Successful application of artificial Intelligence-assisted analysis of invasive pulmonary adenocarcinoma less than 6 mm in size: A case report and literature review. Clin Respir J 19: e70073, 2025.
73. Talebi F, Gregucci F, Ahmed J, Ben Chetrit N, D Brown B, Chan TA, Chand D, Constanzo J, Demaria S, I Gabrilovich D, *et al*: Updates on radiotherapy-immunotherapy combinations: Proceedings of 8th Annual ImmunoRad Conference. Oncoimmunology 14: 2507856, 2025.
74. Suzuki H, Maruya Y, Inomata S, Yamaguchi H, Ozaki Y, Watanabe M, Fukuhara M, Muto S and Okabe N: Clinical significance and future prospects of tertiary lymphoid structure in lung cancer. Gan To Kagaku Ryoho 52: 628-632, 2025 (In Japanese)
75. Jahangir CA, Page DB, Broeckx G, Gonzalez CA, Burke C, Murphy C, Reis-Filho JS, Ly A, Harms PW, Gupta RR, *et al*: Image-based multiplex immune profiling of cancer tissues: Translational implications. A report of the International Immuno-oncology Biomarker Working Group on Breast Cancer. J Pathol 262: 271-288, 2024.
76. Lee EJ, Chung HW, So Y, Kim IA, Kim HJ and Lee KY: Recent advances in PET and radioligand therapy for lung cancer: FDG and FAP. Cancers (Basel) 17: 2549, 2025.
77. Hajikarimloo B, Mohammadzadeh I, Tos SM, Habibi MA, Hashemi R, Hezaveh EB, Najari D, Hasanzade A, Hooshmand M and Bana S: Machine learning in prediction of epidermal growth factor receptor status in non-small cell lung cancer brain metastases: A systematic review and meta-analysis. BMC Cancer 25: 818, 2025.
78. Yu J, Kong X and Feng Y: Tumor microenvironment-driven resistance to immunotherapy in non-small cell lung cancer: Strategies for Cold-to-Hot tumor transformation. Cancer Drug Resist 8: 21, 2025.
79. Shang D, Zhou Z, Shi R, Wang Z, Zhang P, Peng F, Li H, Cheng G, Qin H, Xie Z, *et al*: Nanoparticle-based strategy in CAR-T cell immunotherapy: Challenges, implications, and perspectives. Mol Cancer 24: 281, 2025.
80. Rafii S, Mukherji D, Komaranchath AS, Khalil C, Iqbal F, Abdelwahab SI, Abyad A, Abuhelwa AY, Gandikota L and Al-Shamsi HO: Advancing CAR T-Cell therapy in solid tumors: Current landscape and future directions. Cancers (Basel) 17: 2898, 2025.